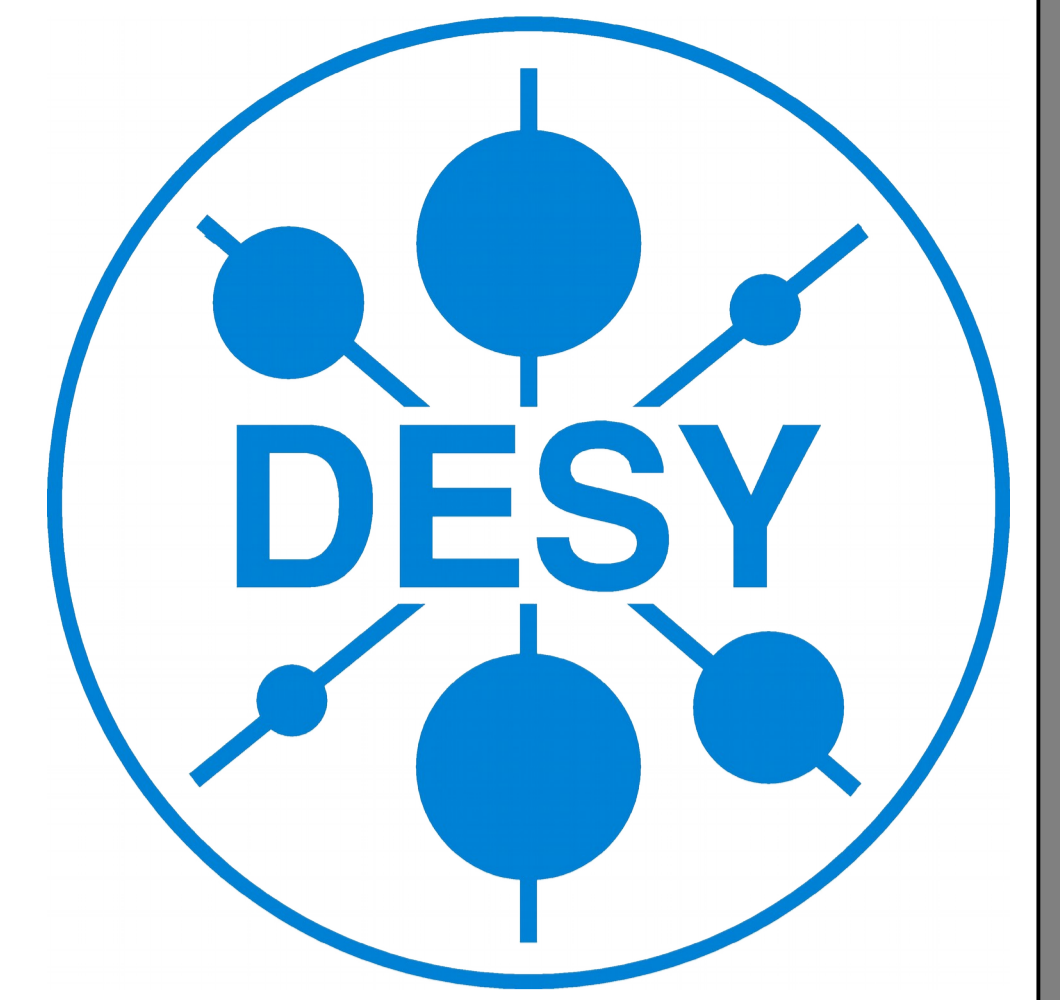
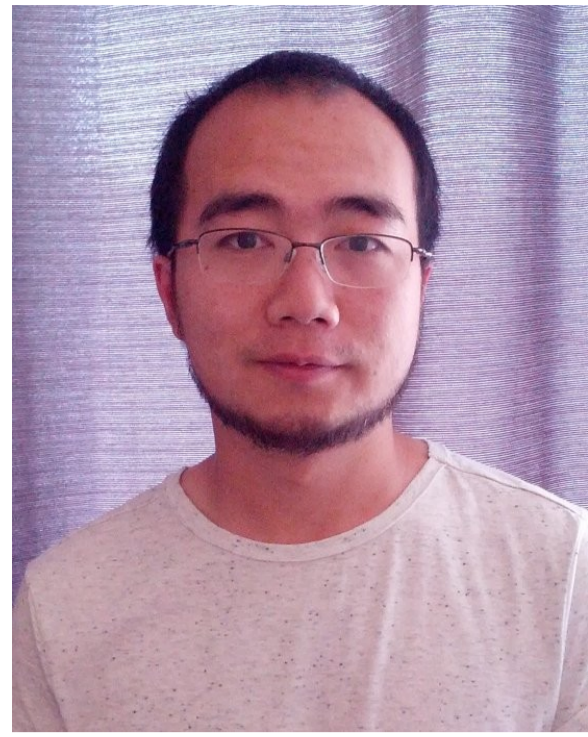


Variability Patterns in Inhomogeneous Jets with Particle Diffusion and Localized Acceleration

Xuhui Chen^{1*}, Martin Pohl¹ and Markus Böttcher²

¹University of Potsdam and DESY, Zeuthen, Germany
²North-West University, South Africa, and Ohio University, USA
 * Email: chenxuhui.phys@gmail.com

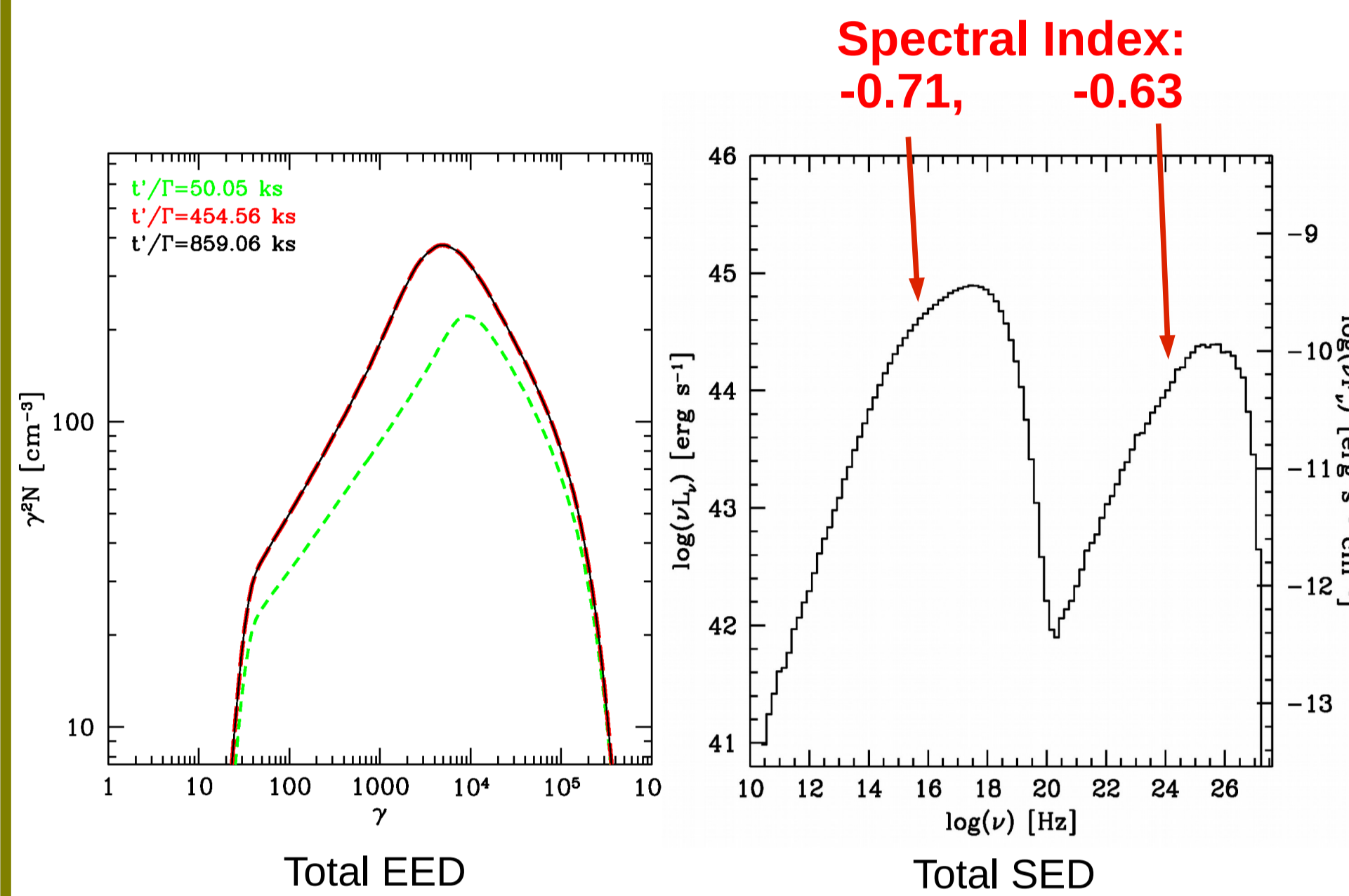


Abstract: We study the acceleration, transport, and emission of particles in relativistic jets. Localized stochastic particle acceleration, spatial diffusion, and synchrotron as well as synchrotron self-Compton (SSC) emission are considered in a leptonic model. To account for inhomogeneity, we use a 2D axi-symmetric cylindrical geometry for both relativistic electrons and magnetic field. If diffusive escape in the emission region is efficient enough, small isolated acceleration regions imbedded within are sufficient to provide the high energy electrons responsible for the spectra of the jet emission. The resulted inhomogeneity in the jet predicts that the SSC spectrum is harder than the synchrotron spectrum. This helps to explain the unexpected hard γ -ray spectra observed in some blazars. When time dependent modeling are considered, random activation of acceleration in small regions in the emission zone produces variability patterns with power spectrum density (PSD) showing red noise profile even though an underlying characteristic time scale does exist. Flux-flux correlation and inter-band lags between X-ray and gamma-ray can change depending on the specifics of the random acceleration.

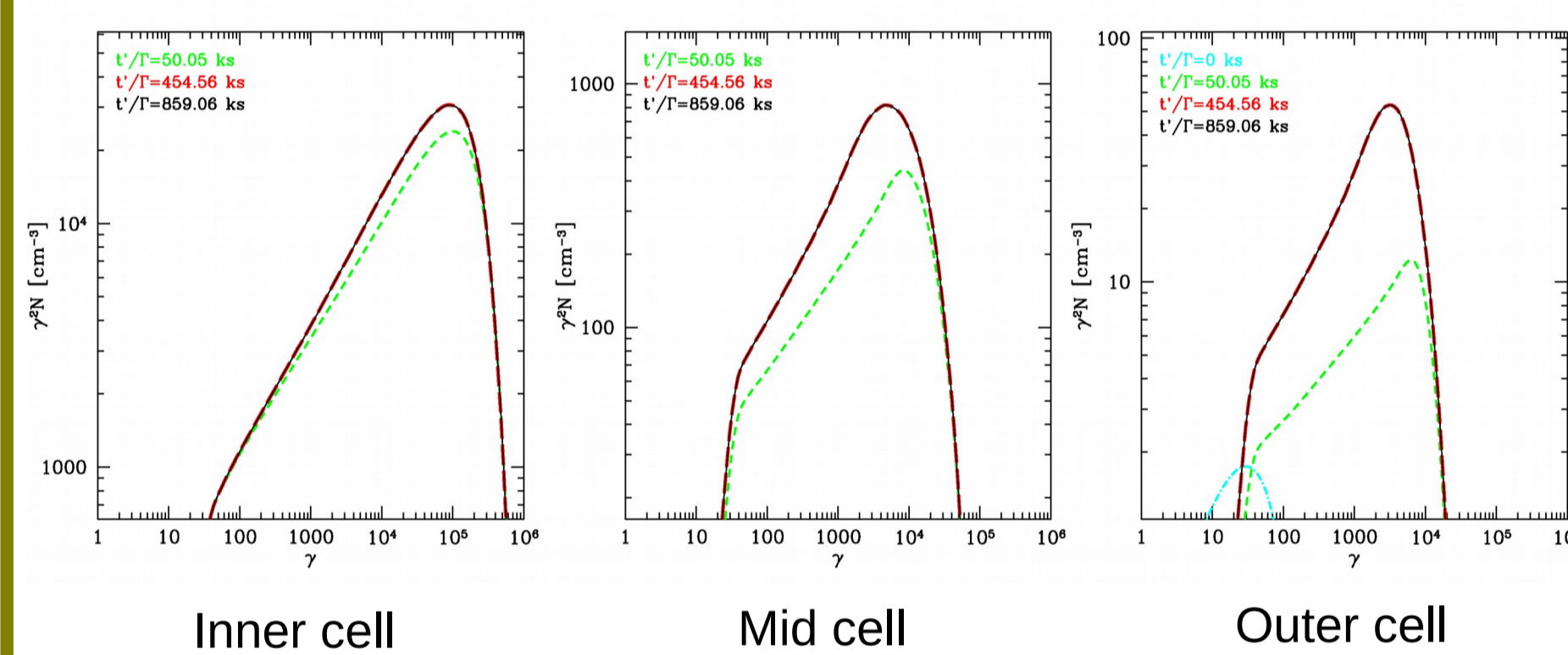
Published Results (Chen et al., 2015, MNRAS)

Acceleration in the center – Steady State Spectrum

The total electron energy distribution (EED) reaches a steady state with a broken power-law distribution. **The SED shows inverse Compton spectrum harder than the synchrotron spectrum.** This is caused by a preference of SSC scattering between high energy synchrotron photons and high energy electrons, both of which are concentrated in the central region.



Below are several sample EEDs in single simulation cells:



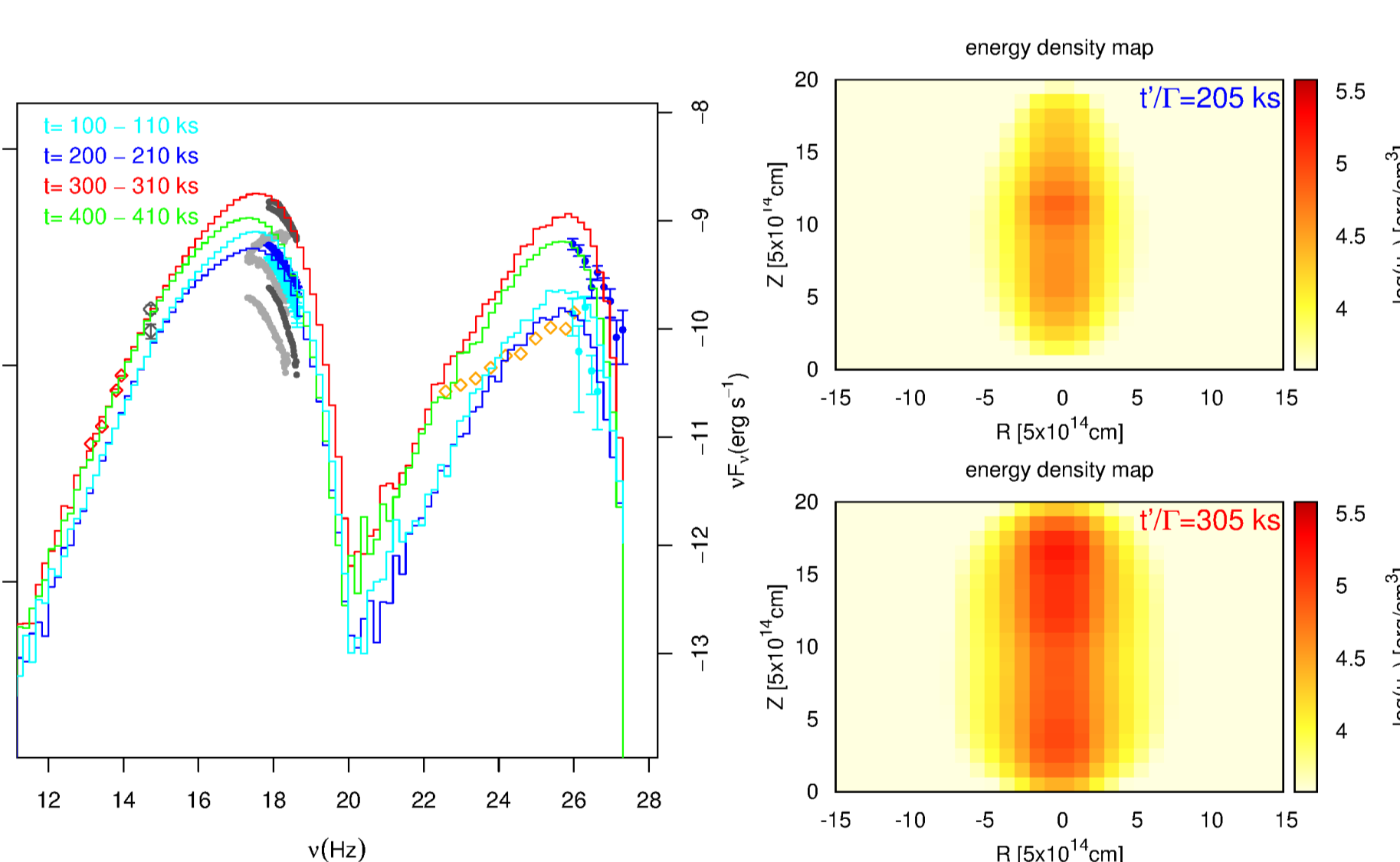
Motivation

- Ultra-fast flares in BL Lacs : small emission region ($\sim 10^{-4}$ pc) (HESS collaboration, 2007)
- FSRQs detected above 100 GeV : far away emission site (\sim pc) (MAGIC collaboration, 2008)

The fastest flares must originate from very small regions because of light crossing time effects. At the same time they should be located relatively far away from the central engine (presumably a black hole). The jet should have expanded considerably by then, therefore **a small high energy region should reside in a relatively large jet.** In order to model such an environment and account for emission on different flare states and at different frequencies, **an inhomogeneous jet model spanning different scales is necessary!**

New Results

Random Acceleration – SED and electron maps



Small acceleration regions along the spine are randomly activated. Dots and circles are observational data points from Mrk 421 (Fossati et al. 2008, Abdo et al. 2011)

Summary:

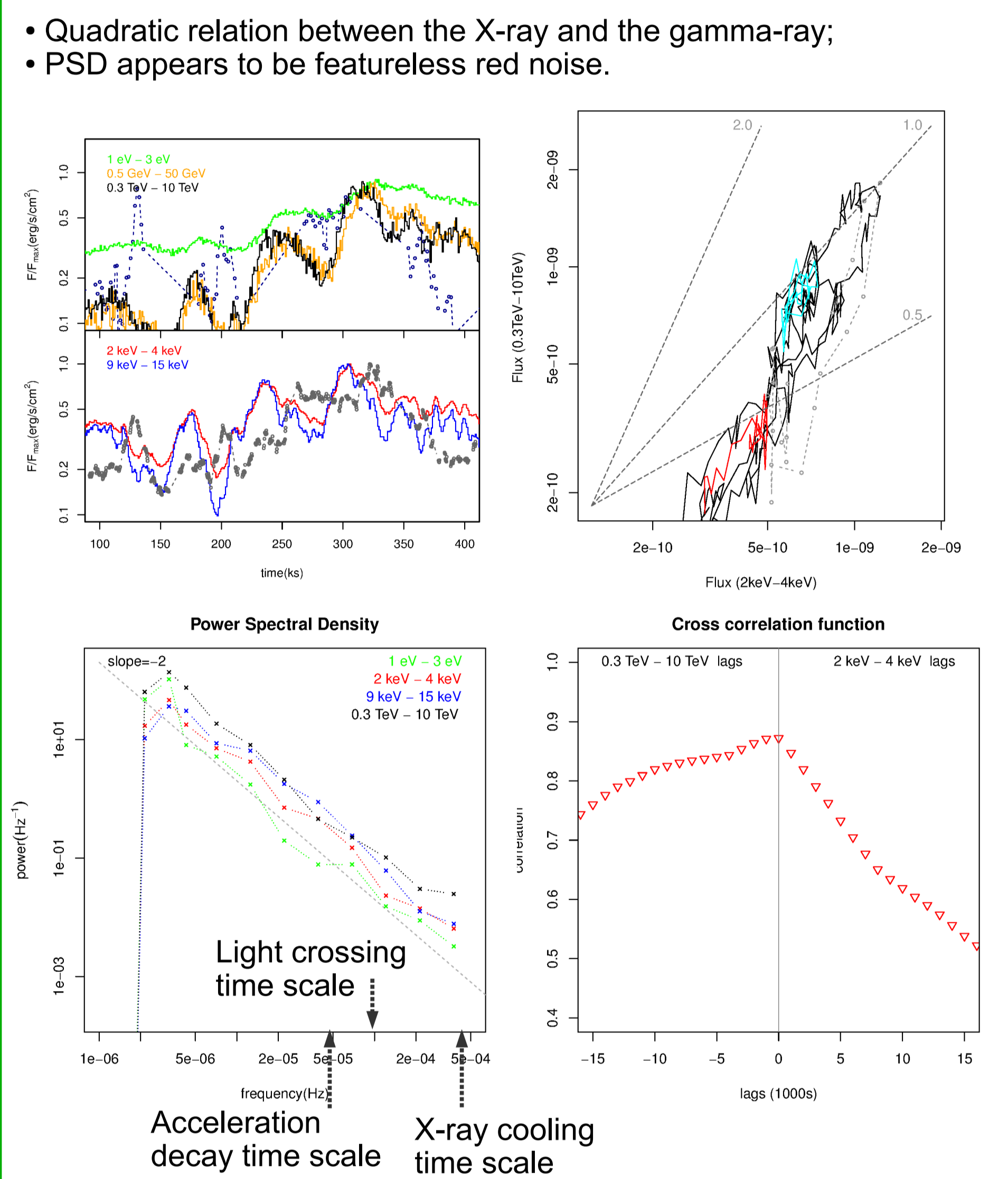
- 1) With acceleration regions much smaller than the emission region, the electrons form broken power-law distributions that adequately reproduce blazar SEDs, with reasonable rate of particle escape;
- 2) The energy dependent inhomogeneity causes the SSC spectrum to be harder than the synchrotron spectrum, and this may help to explain the very hard VHE spectra ($\Gamma < 1.5$) in several blazars (HESS collaboration, 2006);
- 3) The PSDs of the simulated light curves indicate red noise across the time scales considered;
- 4) Variability features such as the flux-flux correlation and cross-correlation function are dependent on the specifics of the random acceleration.

New Results

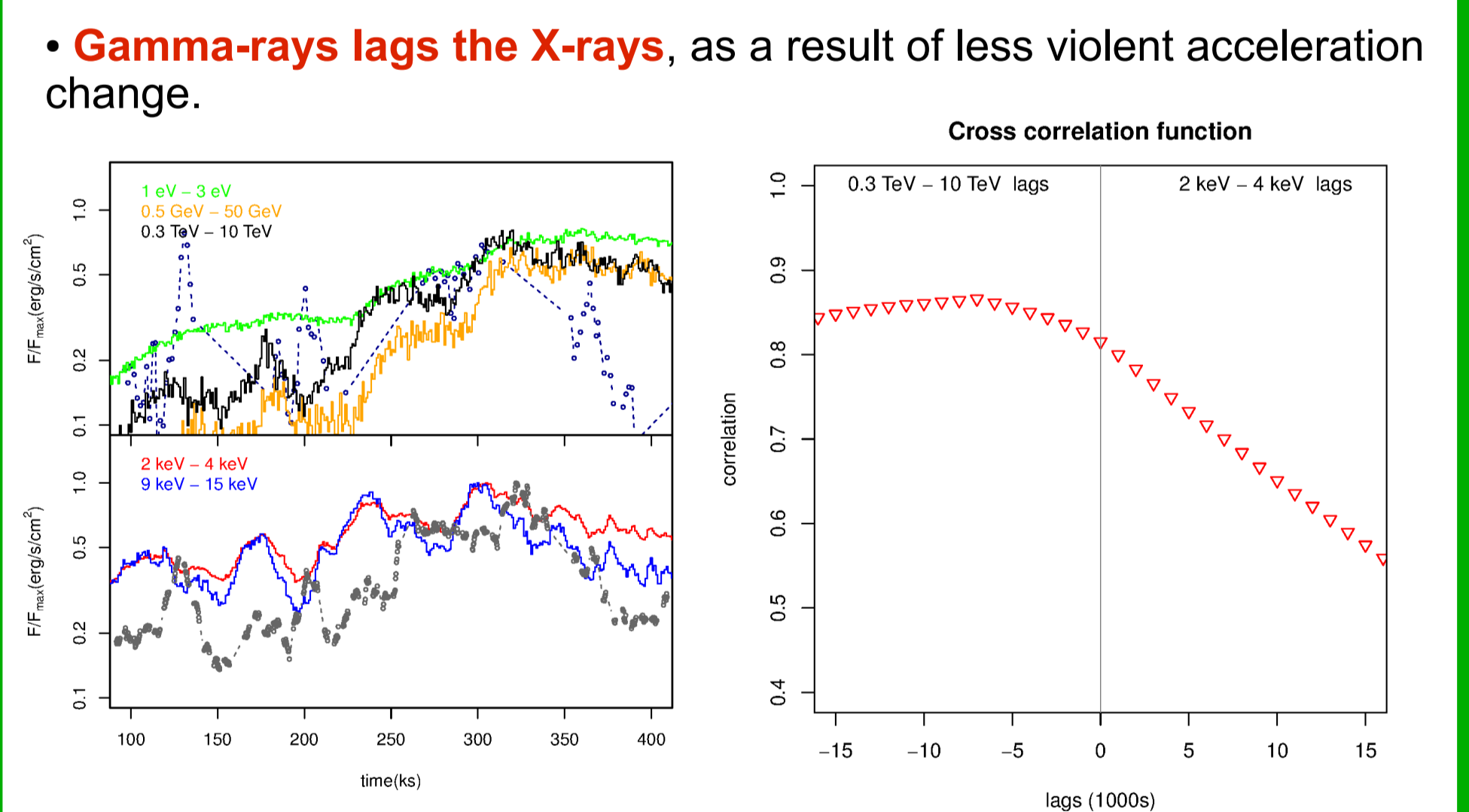
Random Acceleration – Variability Analysis

Grey dots in all the light curves and flux-flux correlation plots are observational data from Mrk 421 in March 2001 (Fossati et al. 2008).

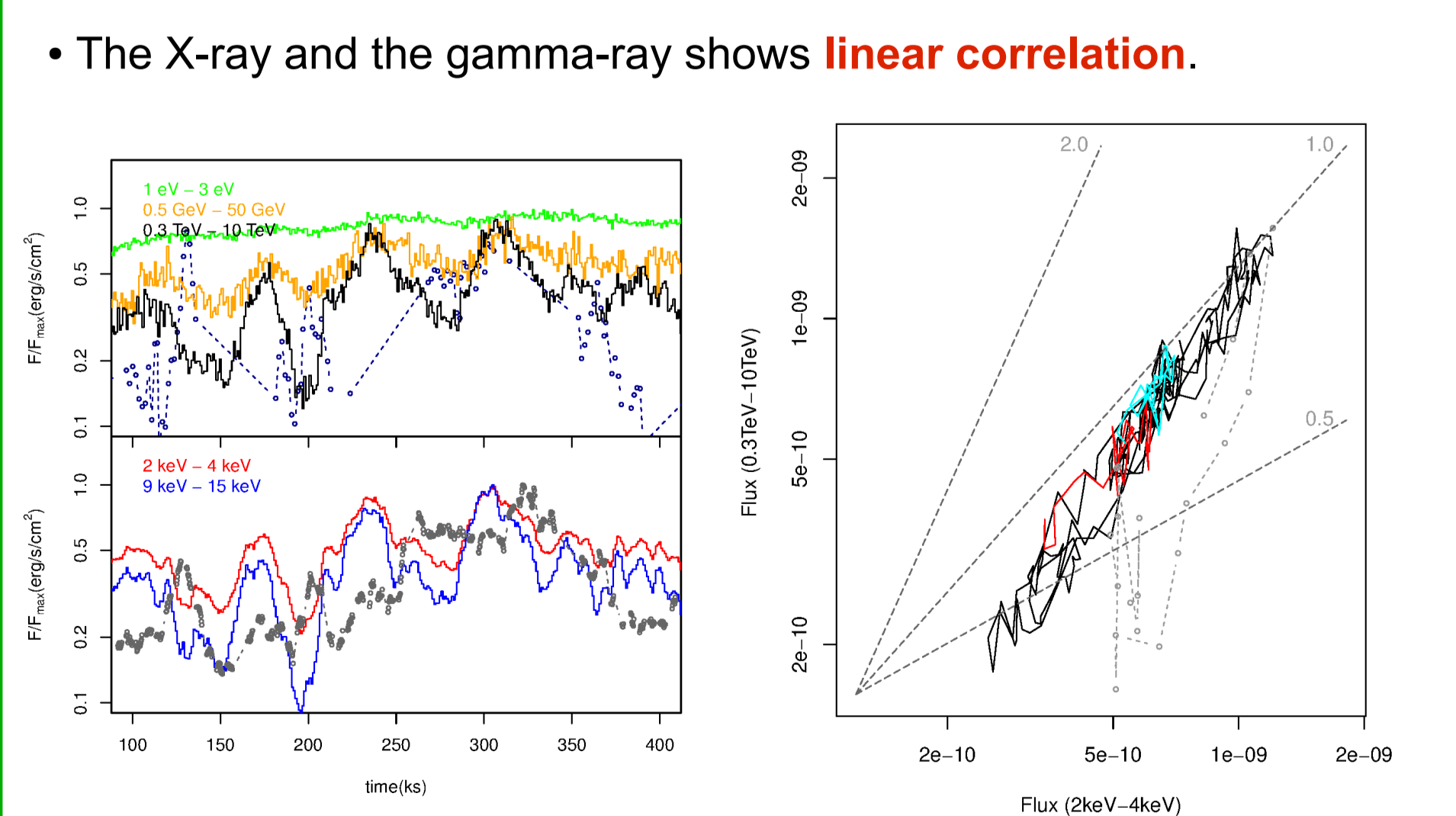
Case 1. The acceleration rates decay on time scale of $T'/\Gamma=20$ ks; Particle injection (at $\gamma \sim 30$) increases with acceleration rate.



Case 2. The acceleration rates decay on time scale of $T'/\Gamma=40$ ks; injection rate increases with acceleration rate.



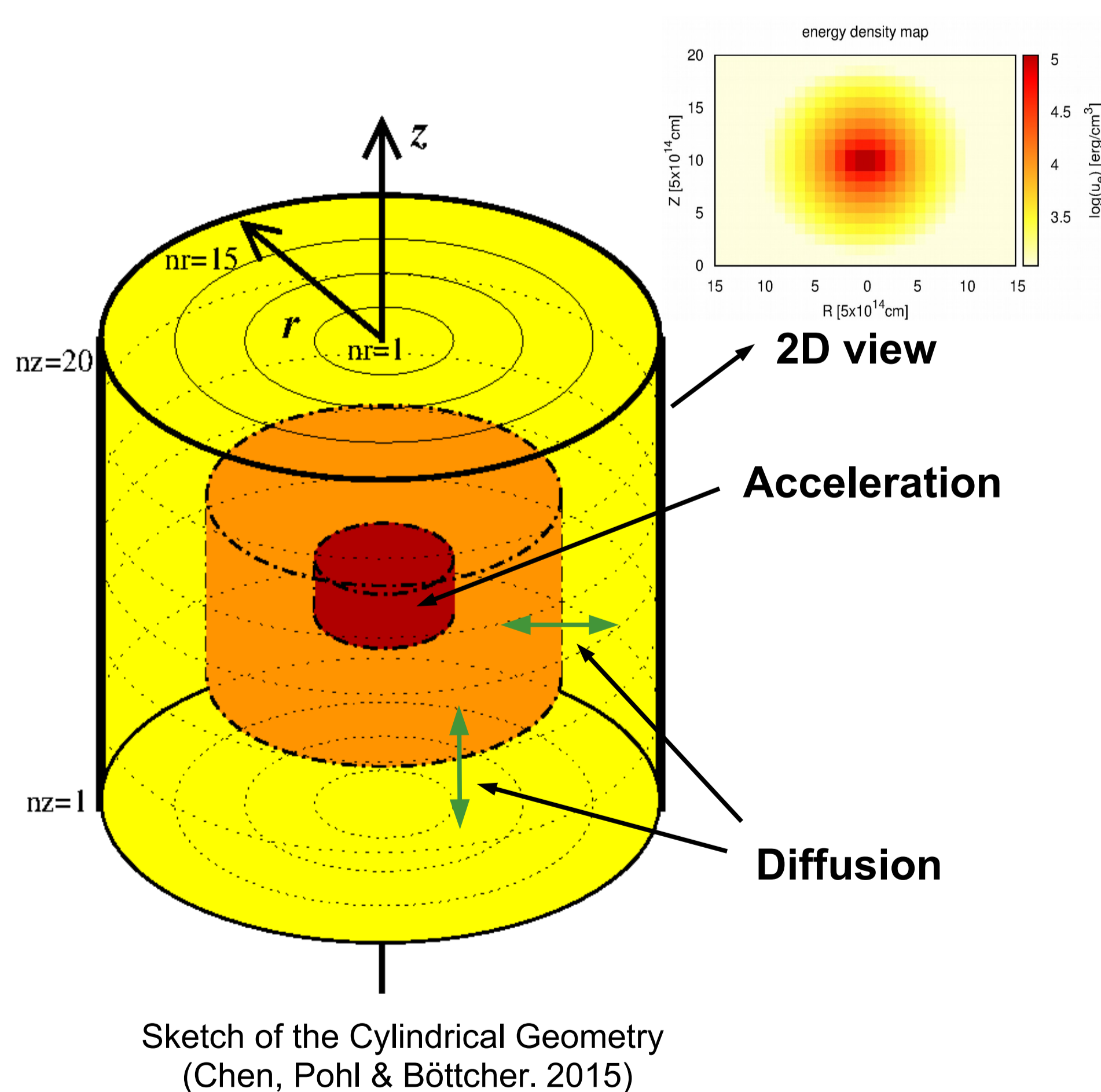
Case 3. The acceleration rates decay on time scale of $T'/\Gamma=20$ ks; injection rate does **not change** with acceleration rate.



References

- HESS collaboration, ApJ, 2007, 664, 71
 HESS collaboration, Nature, 2006, 440, 1018
 MAGIC collaboration, Science, 2008, 320, 1752
 Chen, Fossati, Liang & Böttcher, MNRAS, 2011, 416, 2368
 Chen, Pohl & Böttcher, MNRAS, 2015, 447, 534
 Fossati et al. ApJ, 2008, 677, 906
 Abdo et al. ApJ, 2011, 736, 131

Monte Carlo/Fokker-Planck (MCFP) code



Particle transport equation

$$\frac{\partial n(\gamma, \mathbf{r}, t)}{\partial t} = -\frac{\partial}{\partial \gamma} \left[n(\gamma, \mathbf{r}, t) \dot{\gamma}(\gamma, \mathbf{r}, t) \right] + \frac{\partial}{\partial \gamma} \left[D(\gamma, \mathbf{r}, t) \frac{\partial n(\gamma, \mathbf{r}, t)}{\partial \gamma} \right] + Q(\gamma, \mathbf{r}, t) - \nabla \cdot \left[D_x(\gamma) \nabla n(\gamma, \mathbf{r}, t) \right]$$

Radiative Transfer

Monte Carlo method for inverse Compton scattering.
 All light travel time effects included automatically. (Chen et al. 2011)